Thermal Design of Aeroassisted Orbital Transfer Vehicle Heat Shields for a Conical Drag Brake

W. C. Pitts*
NASA Ames Research Center, Moffett Field, California
and
M. S. Murbach*
Informatics General Corporation, Palo Alto, California

Results from an ongoing study of the performance of thermal-protection systems for a conical, drag-brake-type aeroassisted orbital transfer vehicle (AOTV) are presented. Three types of heat shields are considered: rigid ceramic insulation, flexible ceramic blankets, and ceramic cloths. The results for the rigid insulation apply to other types of AOTVs as well. Charts are presented in parametric form so that they may be applied to a variety of missions and vehicle configurations. The parameters considered include: braking-maneuver heat flux and total heat load, heat-shield material and thickness, heat-shield thermal mass and conductivity, absorptivity and emissivity of surfaces, thermal mass of support structure, and radiation transmission through thin heat shields. Results of temperature calculations show trends with, and sensitivities to, these parameters. The emphasis is on providing useful information in estimating the minimum required mass of these heat-shield materials.

Nomenclature

A = beam cross-sectional area, cm^2
C_p = heat capacity, J/g/K
k = thermal conductivity, mW/cm/K
P.G. = polyimide graphite
$\dot{q}$ = heat flux, W/cm^2
Q = total heat load, J/cm^2
t = heat-shield thickness, cm
α = absorptivity
ρ = density

Subscripts

c = convective
r = radiative
v = visible and ultraviolet radiation to beam
w = wake

Introduction

THERE is a need in future space operations for a vehicle to transfer equipment and supplies between Shuttle/space station altitudes and higher satellite altitudes. The return from the higher orbit can be made either by retropropulsion or aerobraking. The aerobraking option is attractive because a large portion of the retropropulsion fuel-weight savings can be translated into increased payload. The remainder must be used for the aerobraking system. Much work has been done to develop concepts for the design of a lightweight, reliable aerobraking system that will meet all mission requirements.[1,2]

Several types of aerobraking systems have been proposed. They include low-density, zero-lift, inflatable-ballute designs; high-density, lifting-body designs[3,4]; and drag-brake designs.[5] While all of these systems have advantages and disadvantages, there is no consensus on which system will be the most likely choice; therefore, work is continuing on all of them. This paper presents the results of work that is based on a conical drag-brake design.

Presented as Paper 85-1052 at the AIAA 20th Thermophysics Conference, Williamsburg, VA, June 19-21, 1985; revision received March 14, 1986.

*Research Engineer.

The primary emphasis in aeroassisted orbital transfer vehicle (AOTV) studies to date has been on trajectory analysis and braking-maneuver, heat-flux calculations. Very little has been done to study the thermal response of AOTVs to these heat fluxes. This paper addresses the thermal-response problem for a conical aerobrake design. The results of a preliminary study were reported in Ref. 6. In that paper, the heat-shield support structure was not included in the analysis. This paper includes an analysis of the thermal response of the structure. Because the drag brake is still conceptual, a detailed analysis of a specific configuration is not warranted. Instead, a parametric analysis was made on typical drag-brake elements. The intent of this paper is to provide general information on the trends and sensitivity to thermal and physical properties of the system materials. This information will be useful for designers of drag-brake systems, and for developers of thermal-protection materials for fabrication of this type of system. Although the analysis is for a drag-brake system, some of the results are applicable to other types of AOTVs.

Model- and Thermal-Analysis Procedures

The model used to calculate the heat fluxes used in this analysis is shown in Fig. 1. The body is a cylinder with a

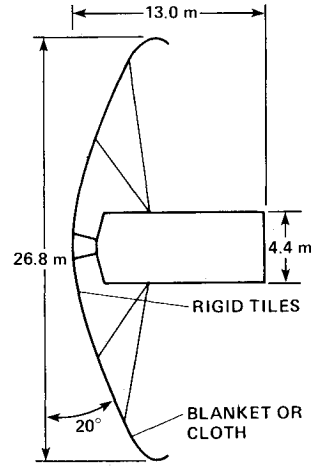

Fig. 1 Proposed conical drag-brake design.

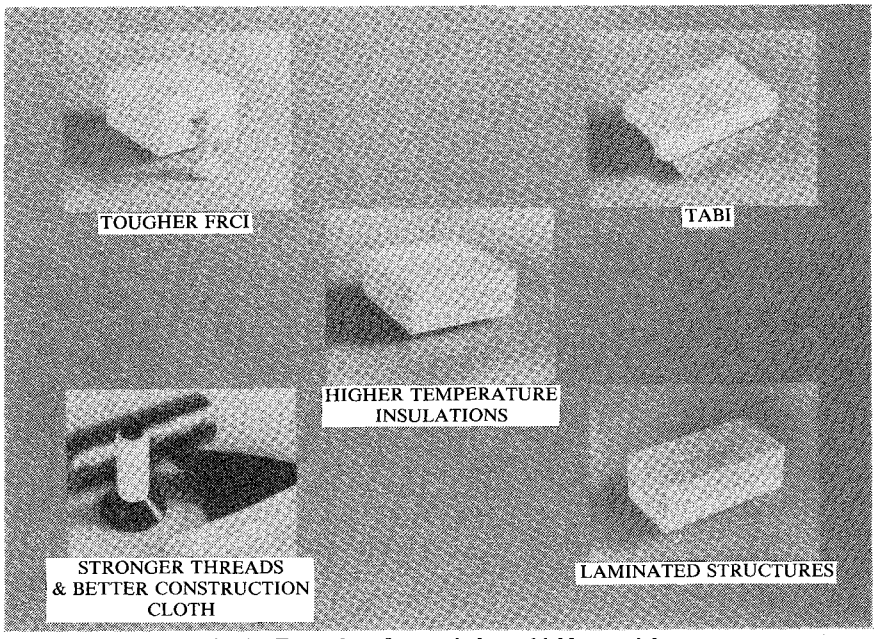

Fig. 2 Examples of ceramic heat-shield materials.

volume suitable for a typical payload with fuel and command and guidance hardware. The entry mass is 11,000 kg. The heat shield is approximately a sphere-cone with an 8-m nose radius. The nominally 70-deg cone is designed to alleviate high edge-heating effects and to minimize hot-gas impingement on the body. The heat-shield support structure is made of I-beam ribs with tubular support struts to the body. The heat shield is made in two sections. For the section outside the radius of the body, ceramic cloth and flexible ceramic blankets were considered. For the section inside the body radius, rigid, low-density, ceramic tiles were used.

Some examples of these three types of heat-shield materials are shown in Fig. 2. The specimens from upper left to lower right are post-Shuttle developments of rigid insulation materials. They are tougher and have higher temperature capability than the LI-900, LI-2200, and FRCI-20-12 developed for the Shuttle. The analysis for the rigid tiles includes all of these. The dark thread at the lower left is silicon carbide, from which Nicalon cloth is made, and the white thread is aluminoborosilicate, from which Nextel cloth is made. By selecting thread size and weave type, these cloths can be tailored to meet a fairly wide range of requirements. Nextel cloth is used for the present analysis. Nicalon has a higher heat-flux capability than Nextel. The blanket option is represented by Tailorable Advanced Blanket Insulation (TABI). This is shown in more detail in Fig. 3. TABI and Advanced Flexible Reusable Surface Insulation (AFRSI) are both used in this analysis.[7,8]

Stagnation-point heat fluxes[9,10] to the conical drag brake shown in Fig. 4 are for a maneuver that brings the vehicle down from geosynchronous orbit to Shuttle orbit. The flow behind the shock was assumed to be in full nonequilibrium. Therefore, this is a conservatively high radiation heat flux. For this analysis, it was assumed that the fabric heat shields absorbed only 20% of the radiation. The remainder was either reflected or, for the thin cloth, partly transmitted through the fabric and scattered diffusely at the back of the heat shield. The convective heat flux is a small fraction of the total flux to the surface, but all of it is absorbed by the surface. In lieu of better information, stagnation-point values were used over the entire surface. This has some physical basis because the radiation component diminishes radially, whereas the convective component increases radially. Wake radiation was also considered. Again, there is no detailed distribution for wake radiation available. An average value was used for the back

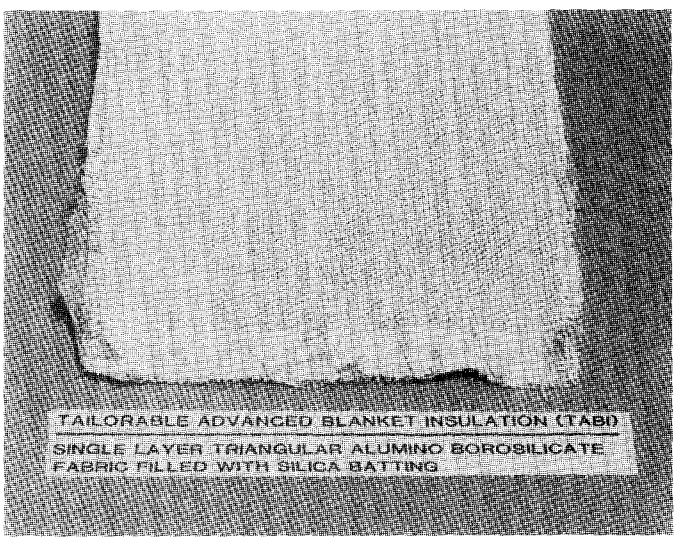

Fig. 3 Detail of Tailorable Advanced Blanket Insulation (TABI).

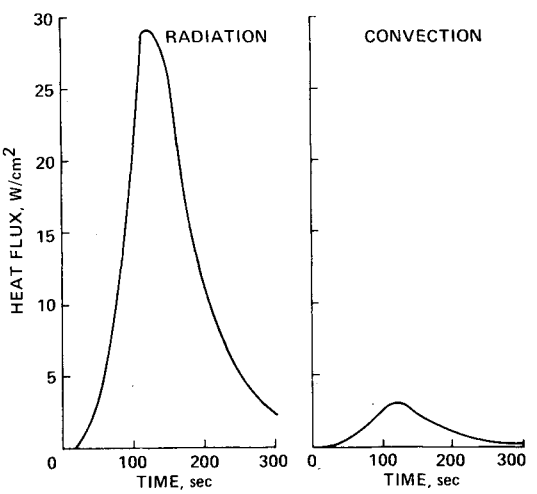

Fig. 4 Braking-maneuver heat flux to drag brake for descent from geosynchronous to Shuttle altitude.

surface of the heat shield and the heat-shield support structure

$$\dot{q}_w = 0.06(\dot{q}_c + \dot{q}_r) \quad (1)$$

This relation is based on an analysis by Park.[11] For the thermal analysis of the rigid tiles, a Fortran program was written for a transient, one-dimensional model to which any time-dependent heat load could be applied to the front surface of the heat-shield tile. Heat was then reradiated forward and conducted inward with a temperature-dependent conductivity. The vehicle structure at the back was assumed to be adiabatic. This assumption will cause the temperatures to be only slightly high because the vehicle structure is assumed to include the local materials that absorb a significant amount of heat during the braking maneuver.

The calculation of the thermal response of the structure behind the flexible-blanket heat shields was done in two steps. First, the temperature on the back of the heat shield was calculated using a one-dimensional transient analysis. Then the thermal response of the support structure was calculated using the aft heat-shield temperatures as a time-dependent radiating source. The models for the calculations were run with and without wake radiation imposed. Several general-purpose, finite-element computer codes were used to perform the thermal-response analysis. The Engineering Analysis Language (EAL)[12] code was used for the one-dimensional analysis of the heat shield. The NASA Structural Thermal Analysis (NASTRAN)[13] code was used for the thermal analysis of the structural elements. The EAL code provides for temperature-dependent thermal conductivity, which is important in calculations related to the heat shield because of the large temperature changes that occur within the material during the braking maneuver. A constant average value for thermal conductivity used for the NASTRAN calculations was satisfactory because, for realistic conditions, the temperature changes within the support structure are relatively small.

For the cloth heat shields, the surface temperature was assumed to be in thermal equilibrium with the total heat flux (front plus wake), with the cloth radiating both fore and aft. The maximum temperature was about 800°C, which is within the temperature limits of Nextel but near the limit of silica for multimission operation. There is a temperature gradient through the cloth, but is is small relative to the temperature magnitude. Two potential concerns with a thin cloth are radiation transmission and the flow of hot gas through the fabric. Some results are shown on the effect of the former, but no analysis was done for the latter. If significant, the flow of the hot gas through the fabric will increase the convective heating of the fabric somewhat and provide an additional heat source for the structure behind the heat shield. This effect will be relatively larger for smaller-diameter drag brakes. Definitive information is lacking on the magnitude of either of these effects.

It has been shown for most cases[6] that, for reasonable thicknesses of heat-shield fabric, the back-surface temperature will be low enough for the fabric to be mounted directly onto the supporting structure, as illustrated qualitatively in Fig. 5. At the other extreme, a thin-cloth heat shield will have an advantage of low fabric weight, but the temperatures are too high for direct mounting.

A proposed means for insulating the structure from a hot-cloth heat shield is depicted in Fig. 6. A typical I-beam support member is shown isolated from a ceramic-cloth heat shield by a strip of ceramic-felt insulation. The insulation could also be placed on the front of the load-bearing cloth to minimize compression of the insulation. If so, the edges of the insulation would be tapered to smooth the outer mold line. Using this model, the I-beam temperature history was calculated for several widths and thicknesses of the insulation. The I-beam size was also varied. An approximate stress calculation indicates that for this size drag brake, the beam height may have to be as much as 15 cm. Temperatures were calculated for I-beam heights ranging from 2.5 to 15 cm. The beams were assumed to be painted white, with an emissivity of 0.8 and a visible range absorptivity of 0.1, unless otherwise specified. The visible radiation comes from the wake gas and from any direct transmission through the thin-cloth heat shield. It is not certain what the transmissivity is for the cloth shields in this environment; therefore, calculations were made for the 0-40% range.

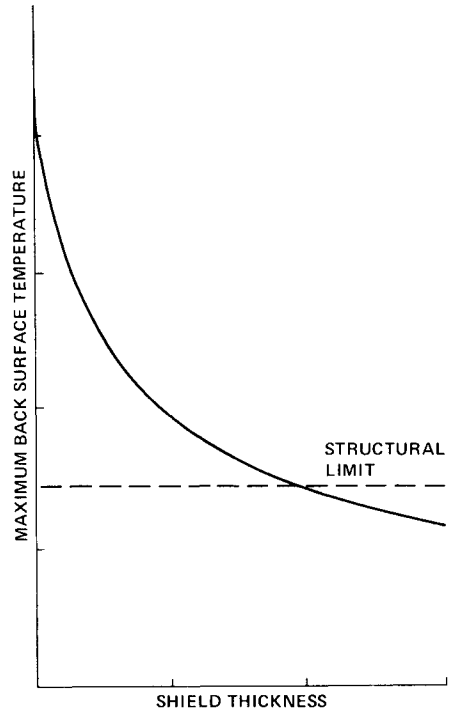

Fig. 5 Maximum back-face temperatures of heat shield during the braking maneuver.

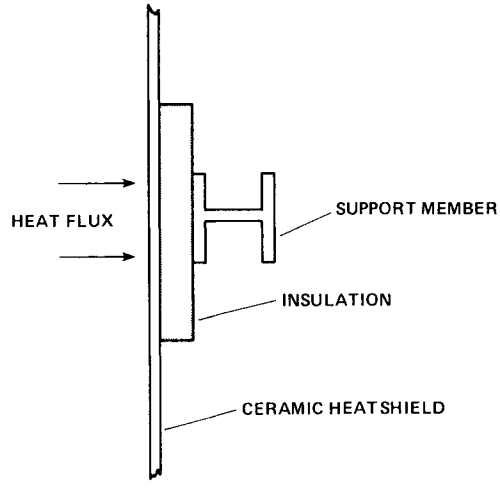

Fig. 6 Model for thermal analysis of the heat shield and support attachment.

Results

As a limiting case, the temperature distribution of a 15-cm polyimide-graphite I-beam attached directly to a thin-cloth heat shield is shown in Fig. 7. The temperatures are about the maximum values for the braking pulse. The temperatures in the upper flange exceed the structural limit of polyimide graphite. For the web and lower flange, the temperatures are all within the structural limits, but the thermal gradients in the lower flange are quite high and may be unacceptable.

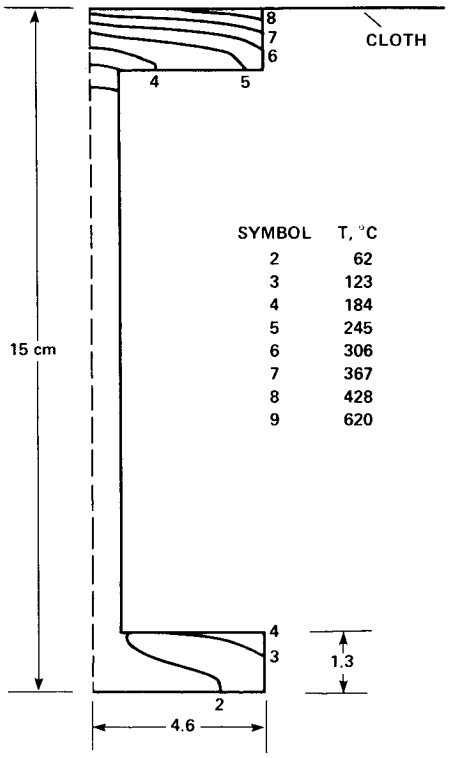

Fig. 7 Polyimide-graphite I-beam temperatures if mounted directly to cloth heat shield.

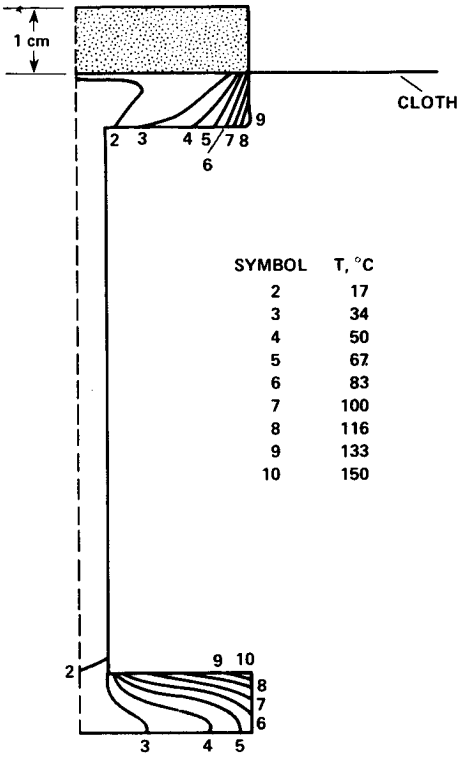

Fig. 8 Polyimide-graphite I-beam temperatures with 1.0-cm ceramic insulation, no overhang.

Figure 8 shows the benefit gained by adding a 1.0-cm-thick ceramic-felt insulation. For the insulation width equal to the flange width, the temperatures are all within the structural limit, although the thermal gradients are still fairly high. If the insulation is extended to 15 cm beyond the I-beam flange, the temperatures become quite benign throughout (Fig. 9). For this case, radiation from the cloth portion of the heat shield is small. The lower-flange hot spot can be eliminated by using a T-beam, if this is desirable.

For all insulated I-beam cases, the maximum temperature is at the upper corner of the lower flange. The view factor from the heat shield to the I-beam is greatest at this point. The temperature at this point will be used as the reference temperature in the summary plots.

A summary of the calculations for the thermal response of the I-beam is shown in Figs. 10-12. In Fig. 10, the maximum temperatures are shown as a function of insulation overhang for several beam depths. For all cases, the temperatures fall off rapidly with increasing overhang. The beam depth and wake radiation both cause significant effects. The temperature rises rapidly as the I-beam depth is reduced.

Figure 11 shows the effect of varying the insulation thickness for a 15-cm overhang. For the zero-thickness limit, the front-surface heat load was applied directly to the I-beam with the same surface characteristics as the cloth. The temperature falls off rapidly as the insulation thickness is increased from 0 to 0.5 cm, where additional thickness becomes relatively ineffective.

Figure 12 shows the sensitivity of the I-beam temperatures to radiation transmission through the cloth heat shield, and to the absorptivity of the I-beam surface for visible radiation. The incident radiation to the heat shield is that shown in Fig. 4. This result is for zero insulation overhang so the I-beam could be protected from the transmitted radiation by adding a moderate amount of overhang. However, the transmission may still be a concern for other support and vehicle structures behind the heat shield.

A summary of the heat-shield mass requirements is shown in Fig. 13 as a function of thickness for the 13.4-m radius drag brake, assuming that the center is protected by a rigid ceramic

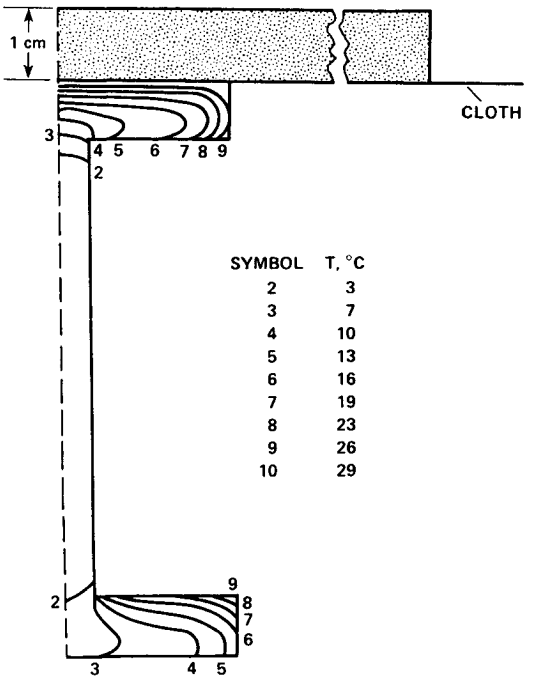

Fig. 9 Polyimide-graphite I-beam temperatures with 1.0-cm ceramic insulation, 15-cm overhang.

insulation. Only the ceramic-fabric masses are shown. Because there are numerous blanket and cloth variations, a mass range is shown for both options. The blanket materials are AFRSI and TABI. The cloths are single and double plies of nominally 0.066-cm-thick Nextel 312 and Nextel 440. The cloth masses include a 0.5-cm-thick insulation, with overhang equal to the I-beam thickness. From strictly the thermal tradeoff shown, the cloth option has a mass advantage. However, the selection of a heat-shield thickness requires an overall system analysis which must await selection of a specific vehicle. For specific

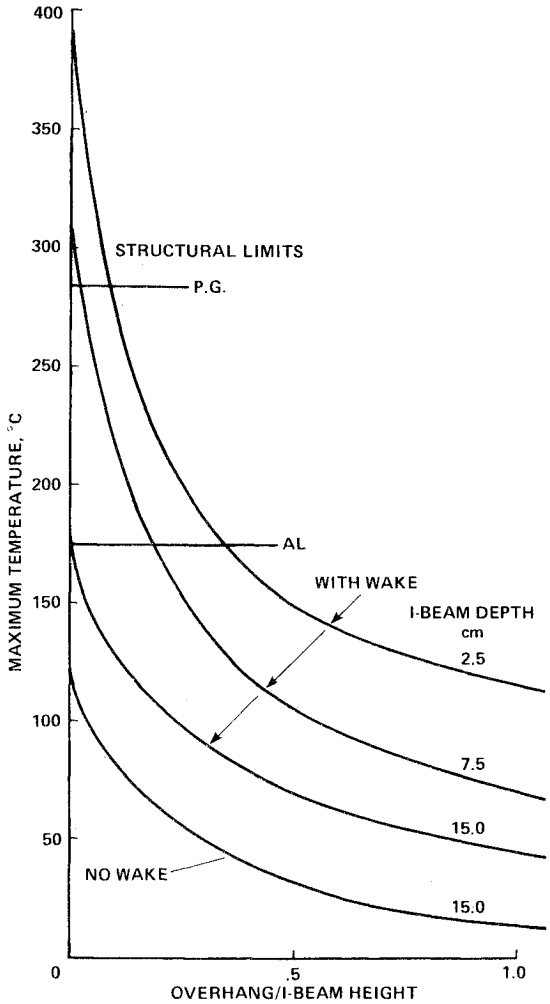

Fig. 10 Maximum polyimide-graphite I-beam temperature with 1.0-cm insulation, $\alpha_v = 0.1$, no transmission.

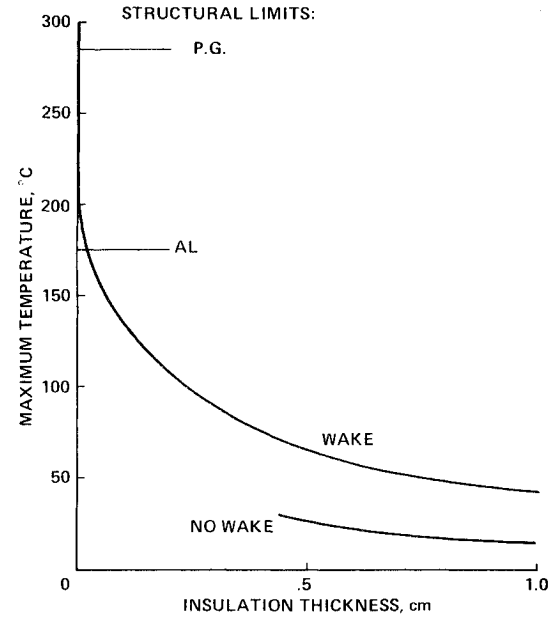

Fig. 11 Maximum polyimide-graphite I-beam lower-flange temperatures with 15-cm insulation overhang, $\alpha_v = 0.1$, not transmission.

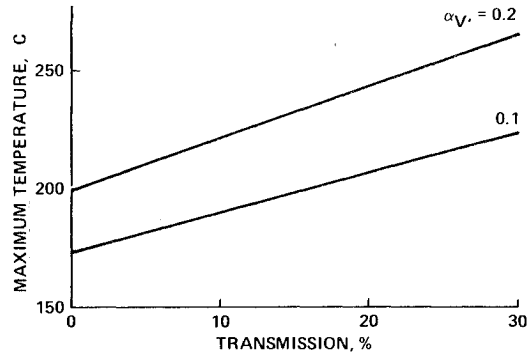

Fig. 12 Effect of radiation transmission on maximum polyimide-graphite I-beam temperature with zero overhang of 1.0-cm insulation.

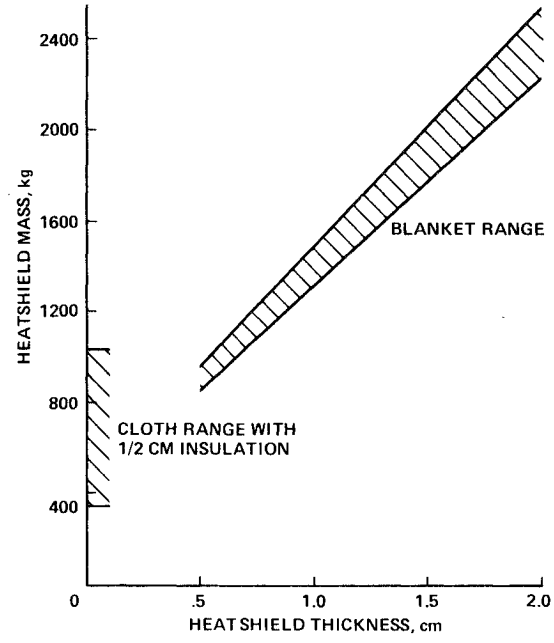

Fig. 13 Heat-shield fabric mass for 13.4-m radius drag brake.

geometries, the radiation transmission and flow-through problems may be of special concern. Also, the required support-structure design may depend on the fabric thickness. It may well be that a thin blanket with a small amount of insulation will provide the minimum mass.

An example of how the choice of heat-shield thickness may depend on the specific vehicle is shown in Fig. 14. In general, the upper half of the heat-shield mass range shown consists of the blankets, and the lower half consists of the cloths, with some overlap. The range broadens parabolically so that the choice of thickness becomes more critical for larger brake radii. The support-structure mass increases even more rapidly with the brake radius. Although the structure mass is only approximate, the trend is qualitatively correct so that the weight advantage shown for smaller brakes is correct. The structure-mass curve is derived by scaling from a structure mass calculated for a vehicle with a 6.7-m brake radius. The payload diameter was kept constant at 2.2 m for all brake radii.

Figure 15 shows the results of thermal-response calculations for low-density, rigid ceramic insulation mounted on a rigid structure. It is arranged as a set of design charts which can be used to estimate the required heat-shield thickness for a variety of conditions. Before the charts are described, the parameters used in the chart should be defined. The structure is defined as an equivalent thickness plate with an effective thermal mass equal to that of all vehicle components that absorb a significant amount of heat in the braking maneuver. It includes the skin, vehicle structure, and bonding materials. Q is the integrated heat load absorbed by the front surface of the

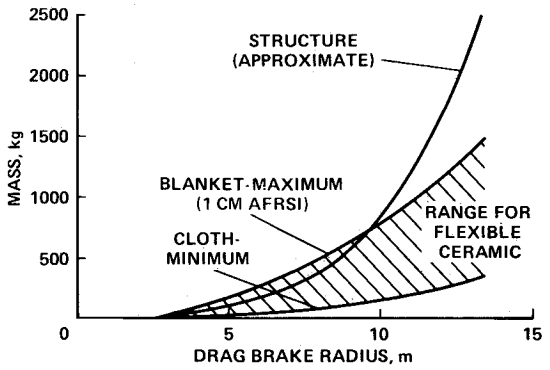

Fig. 14 Dependence of relative component masses upon brake radius.

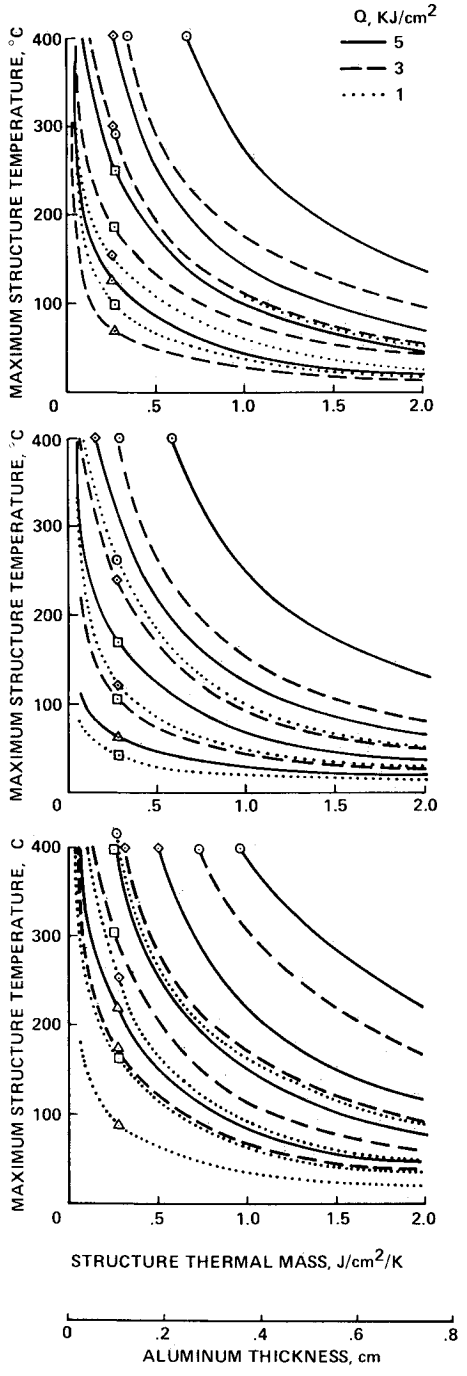

Fig. 15 Sizing chart for ceramic heat shield: a) Low conductivity, $\rho C_p = 0.13$; b) low conductivity, $\rho C_p = 0.33$; c) high conductivity, $\rho C_p = 0.13$.

Table 1 Themal masses

Material	ρC_p
AFRSI	0.13
TABI	0.10
LI-900	0.13
LI-2200	0.33
FRCI-12	0.18
FRCI-20	0.29
Polyimide graphite	2.48
Aluminum	2.82

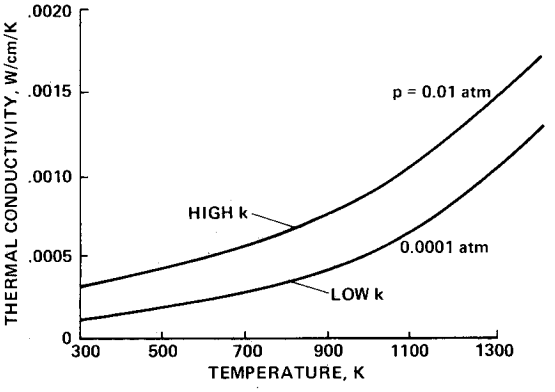

Fig. 16 Thermal conductivity for typical low-density ceramic insulation, LI-900.

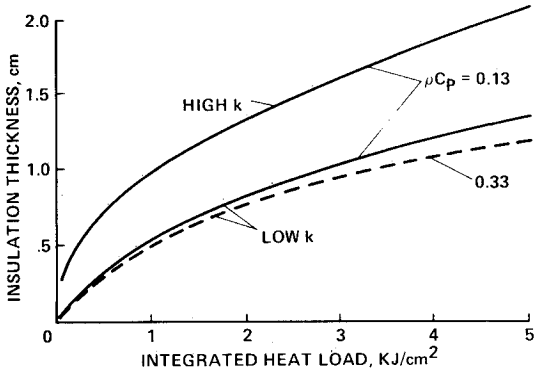

Fig. 17 Sample use of Fig. 15.

heat shield during the braking maneuver. It is assumed that the maximum structure temperature is not significantly dependent upon the shape of the heat pulse, but only on Q. This is reasonable, because the shape and the heat-pulse width are very similar for most braking maneuvers. Also, there are compensating effects between short- and long-duration pulses with the same Q. Detailed calculations to check this assumption showed that for $Q<5$, the maximum structure temperature varied less than 10 deg with reasonable heat-pulse variations.

Three values of Q are used in the chart, each having a different weight curve. There are four curves for each Q, corresponding to the four heat-shield thicknesses designated by the symbols shown in the key.

Each part of the chart is for a different set of material properties. The curves were calculated for insulation thermal masses ρC_p of 0.13 and 0.33, which correspond to LI-900 and LI-2200, respectively. The charts apply to other materials as well. Typical thermal masses for current materials are given in Table 1. The thermal conductivities of the materials are not given in the table, because they depend upon temperature and pressure. Typical thermal conductivity curves are shown in Fig. 16. These are for LI-900 at two pressures, but they are reasonable approximations for all of the insulation materials

discussed herein. Because the maximum atmospheric pressure for most published braking maneuvers is less than 0.0001 atm, the lower curve is the most useful for drag-brake analysis. Nevertheless, a chart is presented for both curves. The curves are labeled "high" or "low" to facilitate coordination with other figures.

A sample of the type of information that can be obtained from Fig. 15 is shown in Fig. 17. To develop this figure, a structure equivalent to 0.2-cm-thick aluminum was chosen and the aluminum structure limit of 180°C was selected for the maximum structure temperature. With this information, the required insulation thickness was read from the chart for several integrated heat loads. It should be pointed out that these charts are general enough to apply to any type of AOTV that has insulation bonded to a rigid structure. This includes FRCI and the blanket materials, AFRSI and TABI, if the maximum surface temperature is low enough.

Concluding Remarks

Results are presented from a study of the performance of the thermal-protection system of an aeroassisted orbital transfer vehicle (AOTV). A specific drag-brake design was used as a point of reference, but most of the results presented have applicability to other drag brakes, and the rigid-tile results have applicability to other types of AOTVs as well. The figures provide information on trends with, and sensitivity to, thermal parameters of the thermal-protection materials. It is hoped that these results will be useful for preliminary design and tradeoff studies for specific AOTV missions as well.

It is difficult to make specific comments that will apply to all missions within the range of this analysis, but some general observations can be made. Three types of heat shields were considered in the analysis: a thin cloth, a thick blanket, and a rigid-tile system. For high-temperature regions (>1000°C), the choice of material is limited to one of the rigid ceramics. For the outer portion of the drag brake, a flexible ceramic heat shield is preferable because it does not require as much dedicated structure as the rigid insulation. However, the mass of this fabric will be significant; therefore, its thickness must be minimized. Results presented show that the mass is less for cloth, including its required insulation from the structure, than it is for a blanket. This is particularly true for large-radii brakes. For smaller brakes, the magnitude of difference is not as large. Other system requirements may dictate the choice between these options, however. The thick blanket provides the advantage of a low-temperature surface for the spacecraft and support structure to view, and minimizes the radiation transmission and hot-gas flow-through problems.

The thermal-protection system will be a significant fraction of the AOTV entry mass. Therefore, its mass should be minimized within the constraints of the overall system. The mass of the thermal-protection system may dictate the form of the vehicle. For example, the mass of the thermal-protection system is strongly dependent upon the vehicle diameter. This may be a factor in the selection of the AOTV size. The results presented herein should be useful in this mass-optimization process.

References

[1]Walberg, G. D., "A Survey of Aeroassisted Orbit Transfer," *Journal of Spacecraft and Rockets,* Vol. 22, Jan.-Feb. 1985, pp. 3-18.

[2]Menees, G. P., "Trajectory Analysis of Radiative Heating for Plantary Missions with Aerobraking of Spacecraft," *Journal of Spacecraft and Rockets,* Vol. 22, Jan.-Feb. 1985, pp. 37-45.

[3]Florence, D. E., "Aerothermodynamic Design Feasibility of a Mars Aerocapture Vehicle," *Journal of Spacecraft and Rockets,* Vol. 22, Jan.-Feb. 1985, pp. 74-79.

[4]Scott, C. D., Reid, R. C., Maraia, R. J., Li, C. P., and Perry, S. M., "An AOTV Aeroheating and Thermal Protection Study," AIAA Paper 84-1710, June 1984; also, *Progress in Astronautics and Aeronautics Series,* Vol. 96, AIAA, New York, pp. 309-337.

[5]Davies, C. B. and Park, C., "Aerodynamics of Generalized Bent Biconics for Aeroassisted, Orbital-Transfer Vehicles," *Journal of Spacecraft and Rockets,* Vol. 22, March-April 1985, pp. 104-111.

[6]Pitts, W. C. and Murbach, M. S., "Thermal Response of an Aeroassisted Orbital-Transfer Vehicle with a Conical Drag Brake," AIAA Paper 84-1712, June 1984; also, *Progress in Astronautics and Aeronautics series,* Vol. 96, AIAA, New York, pp. 361-377.

[7]Goldstein, H. E., "Fibrous Ceramic Insulation," NASA CP-2251, Nov. 1982.

[8]Sawko, P. M., "Flexible Thermal Protection Materials," *Proceedings of Symposium on Advances in TPS and Structures for Space Transportation Systems,* Dec. 1983; also, NASA CP-2315.

[9]Menees, G. P., "Thermal Protection Requirements for Near-Earth Aeroassisted Orbital-Transfer Vehicle Missions," AIAA Paper 83-1513, June 1983; also, *Progress in Astronautics and Aeronautics series,* Vol. 96, AIAA, New York, pp. 257-285.

[10]Menees, G. P., Davies, C. B., Wilson, J. F., and Brown, K. G., "Aerothermodynamic Heating Analysis of Aerobraking and Aeromaneuvering Orbital-Transfer Vehicles," AIAA Paper 84-1711, June 1984; also, *Progress in Astronautics and Aeronautics series,* Vol. 96, AIAA, New York, pp. 338-360.

[11]Park, C., "Problems of Radiative Base Heating," AIAA Paper 79-0919, May 1979.

[12]Marlowe, M. B., Moore, R. A., and Whetstone, W. D., "SPAR Thermal Analysis Processors Reference Manual System Level 16," NASA CR-159162, Vol.I, 1978.

[13]Lee, H. P., "NASTRAN Thermal Analyzer—Theory and Application Including a Guide to Modeling Engineering Problems," NASA TM X-3503, Vol. I, 1977.